CARS Thermometry in Laminar Sooting Ethylene-Air Co-Flow Diffusion Flames with Nitrogen Dilution

Aman Satija[a*], Ziqiao Chang[a], Albyn Lowe[b], Levi M. Thomas[a], Assaad R. Masri[b] and Robert P. Lucht[a]

a) School of Mechanical Engineering, Purdue University, 585 Purdue Mall, West Lafayette, Indiana 47906, USA
b) School of Aerospace, Mechanical and Mechatronic Engineering, University of Sydney, Sydney, Australia.
**Corresponding author: asatija@purdue.edu*

Abstract

Temperature measurements were performed in nonpremixed, sooting jet flames using coherent anti-Stokes Raman scattering (CARS). The jet fluid was ethylene diluted with different concentrations of nitrogen, and the co-flow fluid was dry air. The flames were stabilized on a Yale burner, also known as Smooke/Long burner, and the operating conditions were chosen to match previous experiments on the burner by the Yale group and other research groups. The selected flames have also been identified as target flames by the International Sooting Flame Workshop. CARS measurements of temperature provide insight into the structure of these sooting flames and serve as benchmark data for comparison with computations. A dual-pump vibrational CARS system was used here in order to avoid soot interferences. We were able to obtain high quality CARS spectra in all regions of the flame including the highly sooting regions and near the exit of the fuel nozzle, where the nonresonant modulation of the nitrogen CARS spectrum is strong due to the high ethylene concentrations. The measurements are compared with CFD results in literature and discussed in context of measured soot volume fraction, also, from literature.

Introduction

The formation of particles in combustion systems is receiving considerable attention because soot is a known carcinogen that also plays a role in radiation trapping in the atmosphere as well as the formation of photochemical smog[1]. Due to its negative implications on health and environment, soot/particulate matter emissions are subjected to increasingly stringent regulations which control not only the total mass of particles emitted but also their size distribution. Responding to such restrictions requires a thorough, yet incomplete knowledge of the processes

underlying soot formation and extensive efforts are currently invested to advance predictive capabilities[2]. The International Sooting Flame (ISF) Workshop[3] is one of many venues focusing on the continuing development of accurate soot growth and soot chemistry models[4] which must be validated against benchmark data.[5,6] An understanding of soot chemistry[7] is also important because of the use of combustion for synthesis functional material such as carbon nano-tubes.[8]

A knowledge of temperature fields is key to the understanding and model development of all soot processes from inception to oxidation.[9,10] Temperature, however, is extremely hard to measure reliably in particle-laden flows and applicable diagnostics methods are rather limited. CARS[11,12], NTLAF[13,14], and thermographic phosphors[15] are, perhaps, the most relevant methods each with its own advantages and disadvantages. Absorption spectroscopy has also been applied in Santoro-type flames.[16] Although easy to setup, absorption techniques are inherently path-averaged methods and rely on inversion algorithms to extract temperature. Temperature measurements in Yale burner flames were performed using thermographic phosphors to extract boundary conditions for sooty flames[17] and temperature measurements were performed using an R-type thermocouple in the flame.[18] Thermocouple measurements were not performed within the high-soot region due to the large uncertainties associated with radiative loss from the thermocouples. Thin-filament pyrometry was performed using a color digital camera to obtain temperature measurements[19] over an entire plane. Those measurements compared reasonably with CFD simulations for the 32% and 40% C_2H_4 flames however the comparison was not good for the more sooting C_2H_4 flames.

In this work we have performed temperature measurements using dual-pump vibrational coherent anti-Stokes Raman scattering (DPVCARS) in laminar diffusion flames of ethylene diluted with nitrogen. The Yale burner, which has been selected as a validation platform for the ISF is adopted here as well. An extensive data set including LII[20] already exists for relevant flames. However, CARS measurements of temperature are lacking and this paper attempts to fill this gap in order to provide a complete benchmark data for validation[21] and further development of soot models. Extensive measurements were performed both in radial and axial direction of flame propagation. CARS is a non-linear spectroscopic technique which is relatively insensitive to collisional environment in the flame. Soot interference between CARS signal and emission from C_2 Swan band, in heavily sooting flames, was studied to provide the best selection of

excitation beams.[22,23] The DPVCARS reported here are of high spatial and temporal resolution and the CARS spectra were of high quality even in highly sooting regions of the flames.

Experimental System

The CARS system used in these experiments was modified from a previous CARS system which was used to perform measurements in turbulent flames.[24] The pump laser was not injection seeded and had an overall energy output of approximately 800 mJ/pulse at 532 nm. The center wavelength of the broadband Stokes beam, to generate Raman coherence of N_2, was approximately 607 nm with a bandwidth of approximately 200 cm^{-1}. The center wavelengths for the interchangeable pump and probe beams were near 532 nm and 560 nm. Diffusion flames have steep temperature gradients and it was considered important to obtain high spatial resolution to avoid spatial averaging effects. In order to achieve this, a lens with a focal length of 175 mm was used to focus the CARS beams into the probe volume. The CARS signal was detected using a 1 m long Czerny-Turner spectrometer and a back-illuminated CCD camera (Andor DU420A-BU2). The spatial resolution of the CARS system was determined by monitoring the nonresonant signal from a thin coverslip which was translated along the propagation direction of the laser beams. The FWHM of this axial resolution was approximately 750 µm and the 10% to 10% was approximately 1.25 mm. The spatial resolution orthogonal to the beam propagation is expected to be approximately 100 µm, the same as the beam waist of the 532 nm beam. A high speed mechanical shutter, with an estimated exposure time less than 20 ms, was employed to reduce interference from soot emission and chemiluminescence from the flame. In order to suppress spectral interferences from the pump and the Stokes beams the CARS signal was transmitted across a 16 nm bandpass filter with a center wavelength of 497 nm (Semrock FF01-497/16-25). Figure 1 shows the experimental system with an inset of a laminar C_2H_4-air co-flow diffusion flame stabilized on a Yale burner.

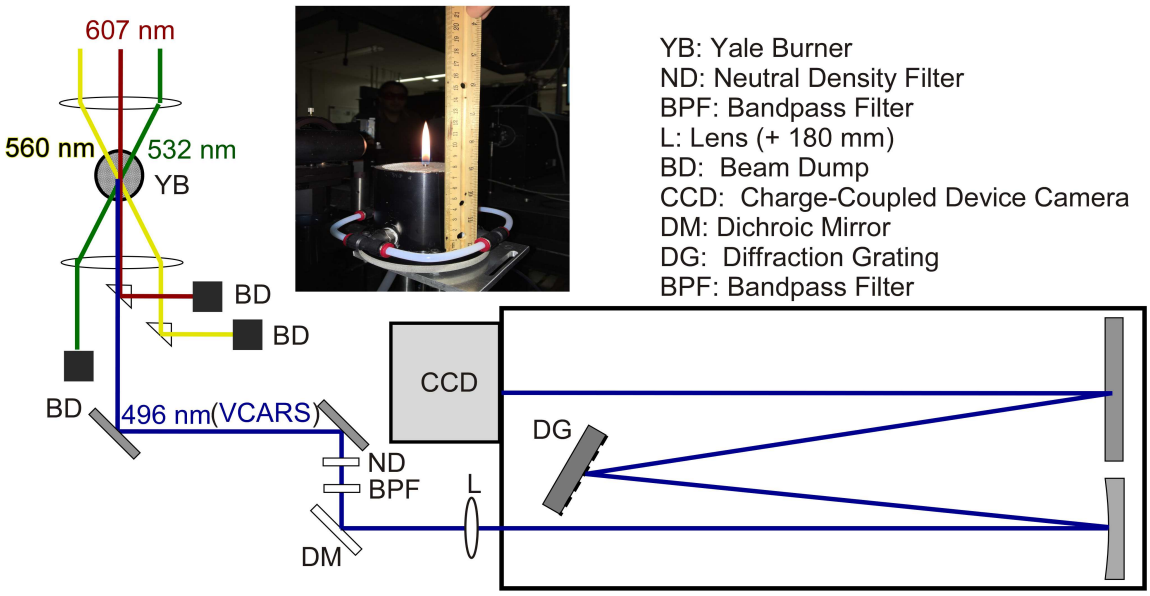

Fig.1: Layout of the CARS thermometry system. A laminar C_2H_4-air diffusion flame stabilized over the Yale burner is shown as an inset.

In the Yale burner the fuel flows from a 4 mm inner diameter center tube with a lip thickness of 0.38 mm. The pipe is surrounded by a co-flow of air with an annular diameter of 76 mm. The fuel and oxidizer cold-flow velocities were matched at 35 cm/s. Rotameters were used to control flow rates for C_2H_4 and N_2 whereas a mass flow controller was used to set the flow rate of the air co-flow. The accuracy of C_2H_4 and N_2 fuel composition was verified by measuring the height of the co-flow diffusion flames and matching it with existing data.[25] Table 1 shows the flow-rate and the visible flame heights for all the "standard" flames. The details of the design of the Yale burner can be found in several manuscripts[17,18] discussing laminar diffusion flames stabilized over a similar Yale burner. The burner was placed on a translation stage and a manual traverse for measurements along the radial and axial directions respectively. CARS measurements were performed along the axial centerline for the standard C_2H_4 non-premixed flames. Typically, 200 single-shots were averaged to obtain an averaged CARS spectrum in the steady flames. The C_2H_4 mole-fraction in the fuel stream was 32%, 40%, 60% and 80%, for the flames investigated, with the balance being N_2. Detailed radial scans were performed for only the 40% C_2H_4 / 60% N_2 flame.

C_2H_4 and N_2 percentage in fuel stream	CH_4 flow rate (lpm)	N_2 flow rate (lpm)	Co-flow air (lpm)	Flame Height (mm)
32/68	0.0832	0.1768	90	27
40/60	0.104	0.156	90	33
60/40	0.156	0.104	90	55
80/20	0.208	0.052	90	77

Table 1: Flow-rates of laminar ethylene-air co-flow non-premixed flames.

Discussion of DPVCARS Spectrum

Measurements were performed along the nozzle centerline with the data points being, typically, 2 mm apart. Near the exit of the nozzle, strong modulation of the resonant signal by the nonresonant C_2H_4 signal was observed. Figure 2 shows the CARS spectrum obtained approximately 4.5 mm above the burner surface for the 40% C_2H_4/60% N_2 flame. As seen in Fig. 1, the bandwidth of the Stokes beam is sufficient to acquire the spectra of both the C=C symmetric stretch and CH_2 bending deformation modes of C_2H_4.

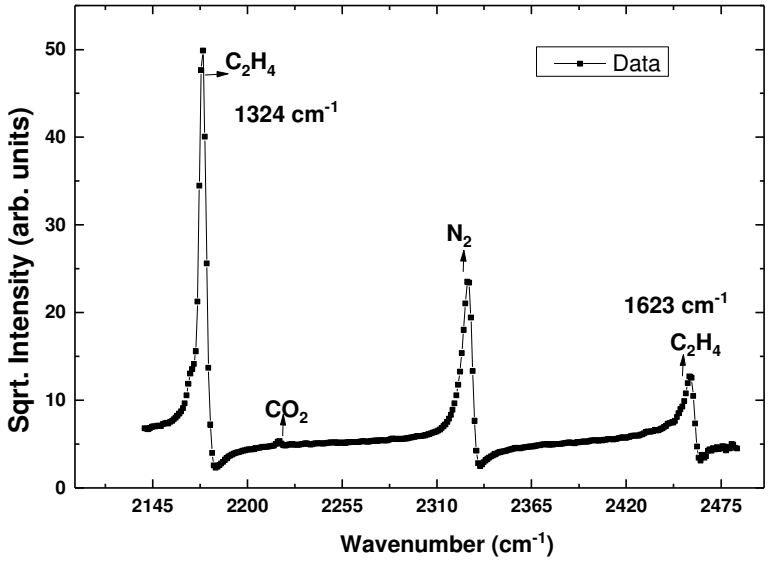

Fig.2: Spectra obtained approximately 4.5 mm above the burner surface in a 40% C_2H_4/60% N_2-air flame.

We used the CARSFT code developed by Palmer[26] and subsequently modified by Cutler and co-workers[27] to fit the CARS spectra. At present we do not have a model for C_2H_4. However, we were able to fit the N_2 spectra even in the presence of strong nonresonant modulation of the CARS spectra. The strong nonresonant modulation is primarily due to the presence of C_2H_4 and this effect decreases away from the burner nozzle. The nonresonant four-wave mixing signal depends on the nonresonant response of the electrons of the species in the probe volume and has a flat spectrum. In the CARSFT code there is a buffer gas whose mole-fraction is equal to one minus the sum of mole-fractions of all other gasses specified in the fitting process. For example, near the exit of the nozzle this buffer gas would be C_2H_4. However, the CARSFT code does not allow us to float the nonresonant susceptibility, corresponding to the buffer gas, as a fitting parameter. Therefore, we allowed the mole-fraction of N_2 to be a floating parameter in order to estimate the nonresonant contribution of the buffer gas. Figure 3 shows spectral fit for N_2 spectra shown earlier in Fig. 1. Good spectral fits were obtained at different locations above the flame and no soot interference was observed even in highly sooting flame conditions. Figures 4 and 5 show CARS spectral fits at different locations. The uncertainty in temperature, based on measurements in Hencken burner flames[28], is estimated to be less than 3% below 1200 K and less than 2% above 1200 K.

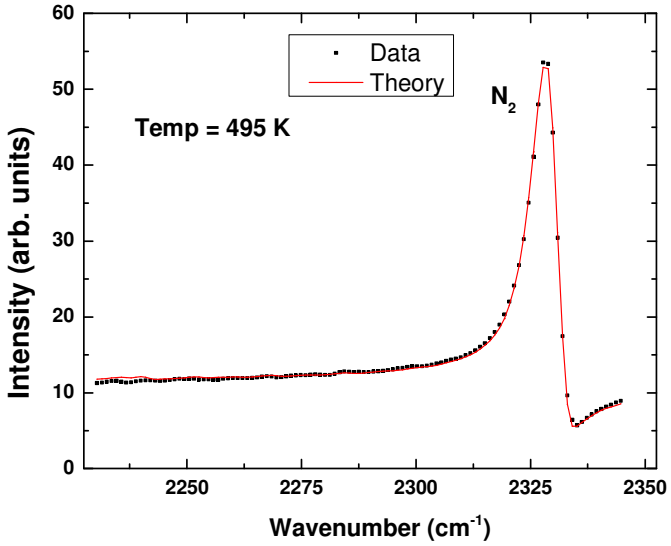

Fig.3: Spectral fit using CARSFT code to N_2 spectrum, extracted from the spectrum, shown in Fig. 1.

The CO_2/N_2 mole-fraction is very sensitive to the spectral fit and a variation of more than 10% can occur for fits of similar quality, thus, leading to large uncertainties. The details for the CARS CO_2 model can be found in literature.[29]

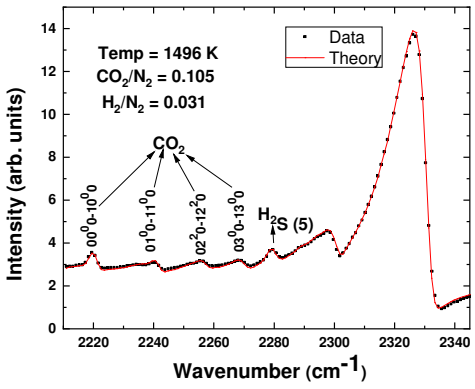

Fig. 4: A 200 shot averaged spectrum approximately 18.3 mm above the burner in the 40% C_2H_4 flame.

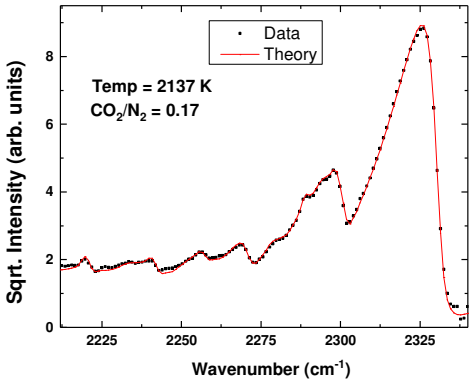

Fig. 5: A 200 shot averaged spectrum approximately 28.3 mm above the burner in the 40% C_2H_4 flame.

Temperature Measurements in Ethylene-Air Co-flow Laminar Diffusion Flames

Previously, measurements using ns-CARS have shown single-shot repeatability, better than 3% at high temperature. We used this feature of CARS to check the non-premixed flames studied here for steadiness. We were able to obtain single-shot spectra with adequate signal to noise ratio and with good spatial resolution. Figure 6 shows a single-shot spectrum obtained in the 60% C_2H_4 flame approximately 60 mm above the burner surface. At this location there is significant mixing between flame gasses and room air. Figure 7 shows a histogram of 290 single-shot spectra at this location. The standard

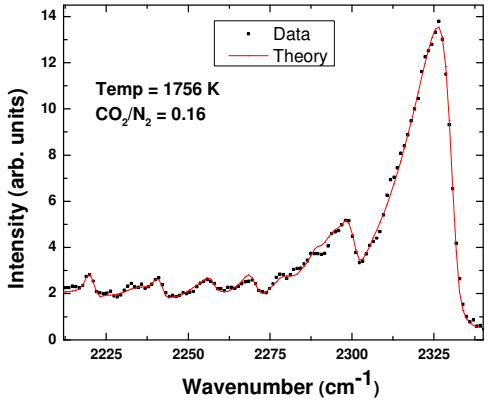

Fig. 6: A single-shot spectrum approximately 60 mm above the burner in the 60% C_2H_4 flame.

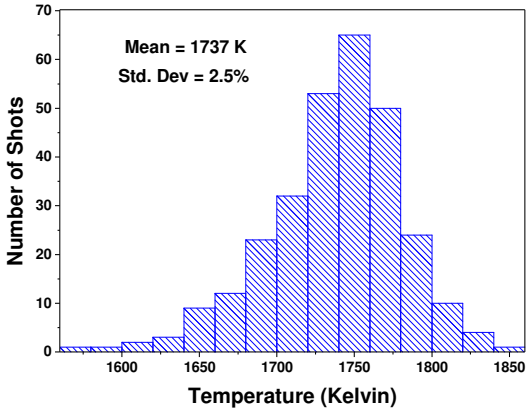

Fig. 7: Histogram of 290 single-shots which indicates the stability of the flames.

deviation of the single-shot measurements is 2.5 % which indicates that the flames are very steady. Such measurements could be useful in quantifying combustion instabilities in other applications.

Figure 7 shows the temperature profiles obtained along the nozzle centerline for the four C_2H_4-air non-premixed flames. It is evident from these measurements that as the percentage of ethylene increases above 40%, the higher sooting propensity leads to higher radiation losses and hence a drop in the peak flame temperature. This is also consistent with the measured chemiluminescence from the flame which is monitored by blocking the Stokes beam. Figure 9 shows the absolute counts of flame emission after subtracting the electronic background of the CCD camera. The flame emission background for all flames was obtained with an optical configuration identical to that of CARS signal detection except that the Stokes beam was blocked. The spatial resolution of the path-averaged flame emission, along the nozzle centerline, is estimated to be less than 1 mm based on the spatial exposure of the CCD sensor (post-binning) and the focal length of the lenses in the detection channel. The absolute counts of the flame

emission are arbitrary since the magnitude of the signal depends on the optical transfer function of the optics in the detection channel, including the bandpass filter and the spectrometer. Table 2 shows the measured peak centerline flame temperature, location of its occurrence, location of the peak soot emission and the peak soot emission intensity normalized to the peak soot emission intensity

which was observed in the 60% C_2H_4-air flame.

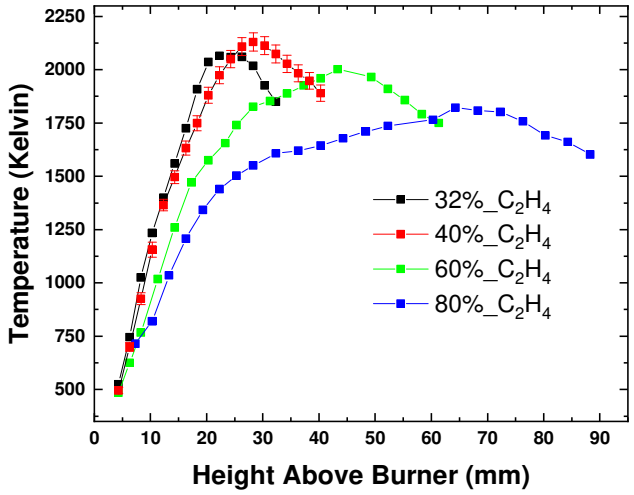

Fig. 8: Measured temperature using DPVCARS thermometry along the nozzle centerline of C_2H_4-air co-flow laminar diffusion flames.

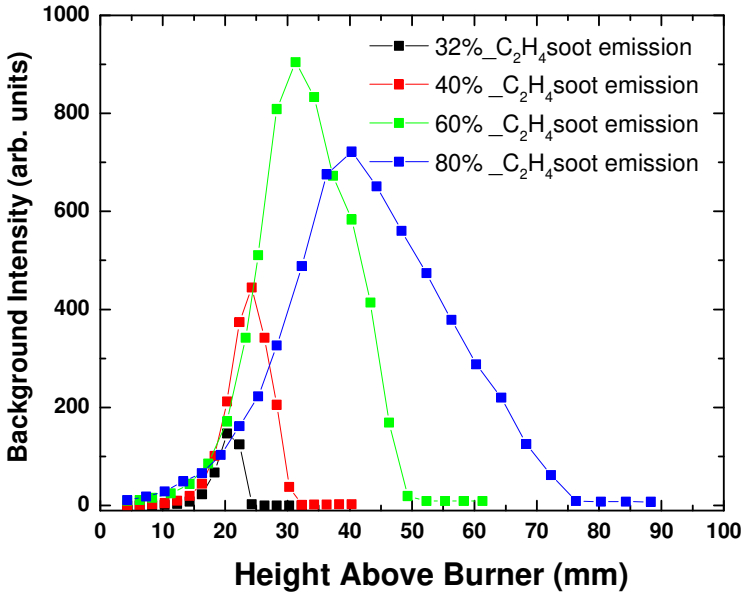

Fig. 9: Measured flame chemiluminescence along the nozzle centerline of

C_2H_4 and N_2 percentage in fuel stream	Measured peak flame temperature(Kelvin)	Height above the burner of the peak flame temperature (mm)	Normalized peak flame emission	Height above burner of peak flame emission (mm)
32/68	2065	22	0.16	20
40/60	2130	28	0.49	24
60/40	2002	43	1	31
80/20	1822	64	0.8	40

Table 2: Summary of measured centerline values of peak CARS temperature and peak flame emission along with the corresponding location.

Figures 10 and 11 shows the axial temperature profiles along with the normalized flame emission profiles. In all cases the location of peak flame emission is upstream of the location of maximum flame temperature. Also, the distance between these two locations increases as the C_2H_4/N_2 ratio increases. For the 60% and 80% C_2H_4 flames there is a slight increase in temperature at downstream locations where the flame emission decreases. CFD calculations

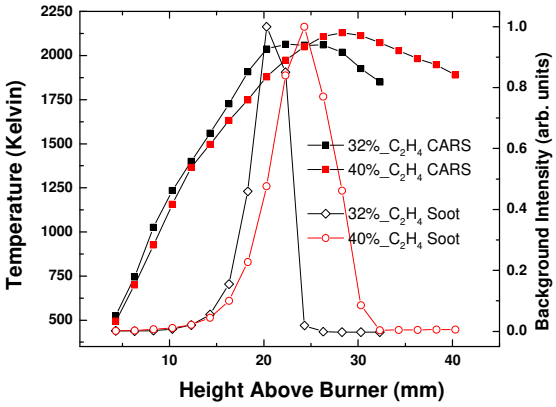

Fig. 10: CARS temperature profiles along with flame emission profiles for the 32% and 40% C_2H_4 flames.

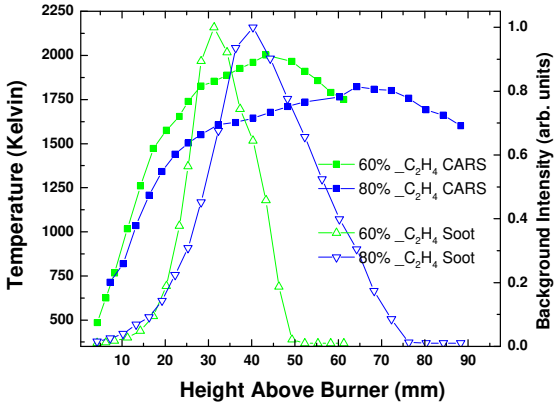

Fig. 11: CARS temperature profiles along with flame emission profiles for the 60% and 80% C_2H_4 flames.

reveal a similar pattern as discussed in a subsequent section.

In order to facilitate comparison with CFD models we also performed detailed radial measurements of temperature in the 40% C_2H_4 flame. These measurements are shown in two

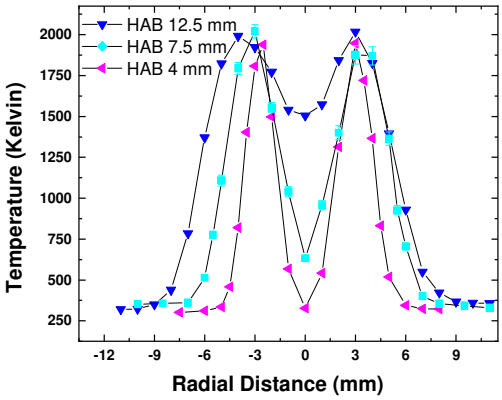

Fig. 12: Radial temperature profiles in the 40% C_2H_4/60% N_2-air laminar co-flow diffusion flames at various heights above the burner.

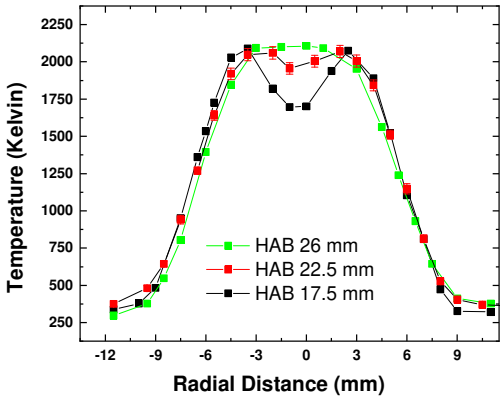

Fig. 13: Radial temperature profiles in the 40% C_2H_4/60% N_2-air laminar co-flow diffusion flames at various heights above the burner.

separate figures, 12 and 13, for easier visualization of data. Good symmetry in the radial profiles demonstrates the repeatability of the CARS measurements even in heavily sooting flames. At lower temperatures the error bars are comparable to the size of the symbol denoting the data.

Comparison of CARS Temperature Measurements with Literature

CARS measurements are discussed in context of key results in literature. Figure 14 shows comparison between the peak flame temperatures, along the centerline of the laminar ethylene-air co-flow diffusion flames, obtained using CARS, thermocouple and numerical simulation.[18] The adiabatic flame temperature is also plotted. The difference in CARS peak temperature and adiabatic flame temperature provides an approximate measure of heat loss due to soot radiation. Thermocouple measurements were only reported outside the soot forming region whereas CARS measurements were performed throughout the flame. The CARS measurements and the thermocouple measurements are in good agreement, especially for the peak flame temperature, as shown in Figs. 15 and 16.

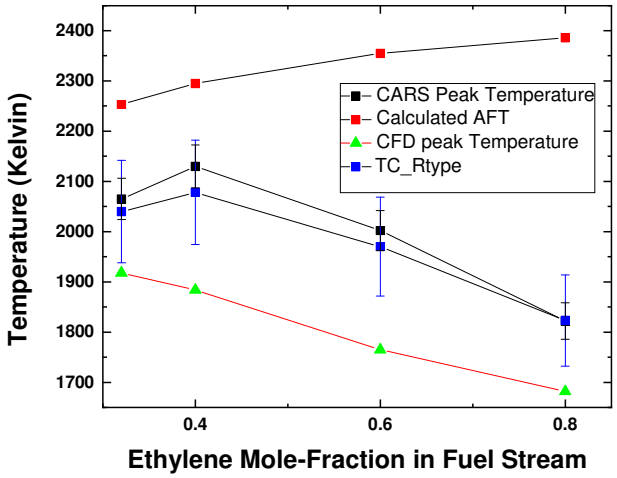

Fig. 14: Comparison between CARS measurements and previous experimental and numerical work. The R-type thermocouple measurements and CFD results were obtained from Smooke et al. (2004).[18]

Temperature profiles using CARS measurements are also compared against the CFD results from the same paper.[18] The temperatures were extracted, from the CFD manuscript, by digitization. A comparison, only for the axial temperatures of the 40% and 80% flames, is shown in Figs. 15 and 16. This comparison illustrates the large discrepancy between experiment and simulations and suggests that the soot models need further development. It is to be noted that, in Fig. 16, the CFD model predicts an increase in temperature, at almost the same location as CARS near 60 mm which coincides with a decrease in flame emission. The reader can find the details on the soot model used by referring to the CFD paper.

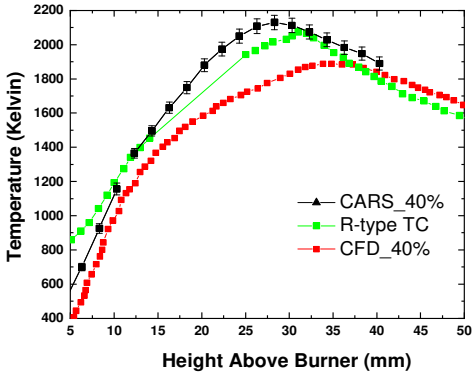

Fig. 15: Comparison between CARS and previously performed thermocouple measurements and CFD calculations, for the 40% C_2H_4 flame, along the nozzle centerline. The R-type thermocouple measurements and CFD results were obtained from Smooke et al. (2004).[18]

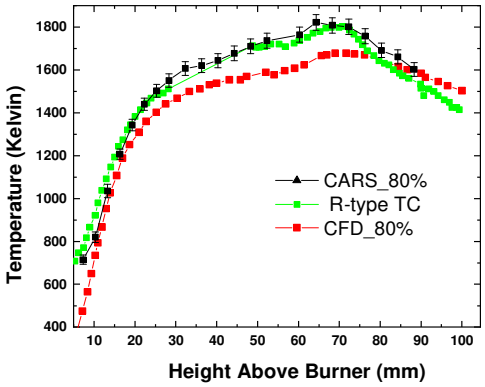

Fig. 16: Comparison between CARS and previously performed thermocouple measurements and CFD calculations, for the 80% C_2H_4 flame, along the nozzle centerline. The R-type thermocouple measurements and CFD results were obtained from Smooke et al. (2004).[18]

Path-averaged flame emission measurements were obtained via the CARS detection channel. These measurements are compared against centerline soot volume fraction (CSVF) measurements previously obtained using laser induced incandescence (LII) measurements.[20] It is to be noted that flame emission depends on the SVF, blackbody temperature of the soot and the flame-emission (this work) would be path-averaged across the flame, therefore, this comparison is qualitative. Table 3 shows the peak location of the flame emission, CSVF and the axial-distance over which the soot emission is dominant.

The peak location of SVF from LII measurements, for the 60% and 80% C_2H_4 flames, is at the edge of the flame whereas for the 32% and 40% C_2H_4 flames it is along the nozzle centerline. Consequently, for the 32% and 40% C_2H_4 flames the peak location of CSVF and flame emission measurement (this work) matches closely however this is not the case for 60% and 80% cases. Along the nozzle centerline, the 32% and 40% C_2H_4 flames have a distinct peak in SVF whereas

the 60% and 80% C_2H_4 flames exhibit a plateau over which the SVF is fairly constant. Figure 17 shows the temperature profiles and CSVF for the 40% and 60% flames. The peak flame temperature occurs after the CSVF begins to decrease. This is consistent with results shown in Figs. 10 and 11. The CSVF for the 40% flame is multiplied by 4 for the sake of comparison against temperature measurements.

C_2H_4 and N_2 percentage in fuel stream	Height above the burner of peak flame emission in our measurements (mm)	Height above the burner of peak CSVF from literature (mm)	Distance over which flame emission (this work) is greater than 20% of peak centerline emission (mm)	Distance over which CSVF is greater than 20% of peak centerline emission from literature (mm)
32/68	20	19	7	5
40/60	24	24	11	9
60/40	31	32-39	26	21
80/20	40	40-59	46	37

Table 3: Peak centerline flame emission from this work and CSVF measurements from Smooke et al. (2005).[20]

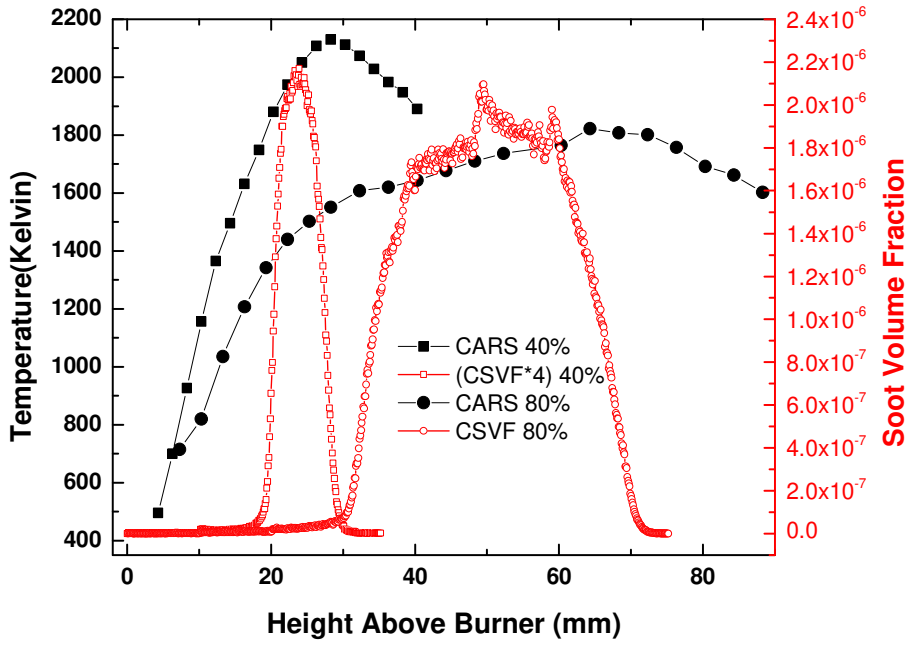

Fig 17: Peak flame temperature is reached after CSVF begins to decrease. The CSVF of 40% C_2H_4 flame was multiplied by 4 for a better comparison with CARS temperature. The R-type thermocouple measurements and CFD results were obtained from Smooke et al. (2005).[20]

Summary and Conclusions

Temperature measurements using DPVCARS thermometry were performed in C_2H_4-air co-flow diffusion flames stabilized over the "Yale" burner. Good spectral fits were obtained to the experimental spectra even in regions of strong nonresonant modulation near the exit of the burner nozzle. No interference was observed in the CARS spectrum in highly sooting regions of the flame. Detailed CARS measurements provided in this manuscript will serve as benchmark data for validation of soot-models in combustion. For the centerline flame temperatures there is reasonable agreement between the thermocouple measurements and the CARS measurements. However, the CFD temperature profiles were considerably different from the measured CARS temperatures.

Acknowledgements

Funding for this research program was provided by the U.S. Department of Energy, Division of Chemical Sciences, Geosciences and Biosciences, Grant No. (DE-FG02-03ER15391). The University of Sydney Combustion Group is supported by the Australian Research Council.

References

[1] B. R. Stanmore, J. F. Brilhac, P. Gilot, The oxidation of soot: a review of experiments, mechanisms and models, Carbon, 39 (2001) 2247-2268.

[2] H. A. Michelsen, C. Schulz, G. Smallwood, S. Will, Laser-induced incandescence: Particulate diagnostics for combustion, atmospheric, and industrial applications, Prog. Ener. Combust. Sci. 51 (2015) 2-48.

[3] International Sooting Flame Workshop, Pressurized Flames and Sprays, 2015, (http://www.adelaide./cet/isfworkshop/data-sets/pressurised/). Accessed: October, 18th, 2015

[4] H. Richterm J. B. Howard, Formation of polycyclic aromatic hydrocarbons and their growth to soot.-a review of chemical reaction pathways, Prog. Ener. Combust. Sci. 26 (2000) 565-608.

[5]A. E. Karatas, O. L. Gulder, Effects of carbon dioxide and nitrogen addition on soot processes in laminar diffusion flames of ethylene-air at high pressures, Fuel 200 (2017) 76-80..

[6] A. M. Vargas, O. L. Gulder, Pressure dependence of primary soot particle size determined using thermophoretic sampling in laminar methane-air diffusion flames, Proc. Combust. Inst. 36 (2017) 975-984.

[7] A. Abdelgadir, I. A. Rakha, S. A. Steinmetz, A. Attili, F. Bisetti, W. L. Roberts, Effects of hydrodynamics and mixing on soot formation and growth in laminar coflow diffusion flames at elevated pressures, Combust. Flame 181 (2017) 39-53

[8] P. Gopinath, J. Gore, Chemical kinetic considerations for postflame synthesis of carbon nanotubes in premixed flames using a support catalyst, Combust. Flame 151 (2007) 542-550.

[9] K. P. Geigle, Y. Schneider-Kuhnle, M. S. Tsurikov, R. Hadef, R. Luckerath, V. Kruger, W. Stricker, M. Aigner, Investigation of laminar pressurized flames for soot model validation using SV-CARS and LII, Proc. Combust. Inst. 30 (2005) 1645-1653.

[10] M. C. Weikl, T. Seeger, M. Wendler, R. Sommer, F. Beyrau, A. Leipertz, Validation experiments for spatially resolved one-dimensional emission spectroscopy temperature measurements by dual-pump CARS in a sooting flame, Proc. Combust. Inst. 32 (2009) 745-752

[11] S. Roy, J. R. Gord, A K. Patnaik, Recent advances in coherent anti-Stokes Raman scattering spectroscopy: Fundamental developments and applications in reacting flows, Prog. Ener. Combust. Sci. 36 (2010) 280-306.

[12] F. Beyrau, T. Seeger, A. Malarski, A. Leipertz, Determination of temperatures and fuel/air ratios in an ethene-air flame by dual-pump CARS, J. of Raman Spectrosc. 34 (2003) 946-951.

[13] P. R. Medwell, Q. N. Chan, P. A. M. Kalt, Z. T. Alwahabi, B. B. Dally, G. J. Nathan, Development of temperature imaging using two-line atomic fluorescence, Appl. Opt. 48 (2009) 1237-1248.

[14] Z. Sun, B. Dally, G. Nathan, Z. Alwahabi, Effects of hydrogen and nitrogen on soot volume fraction, primary particle diameter and temperature in laminar ethylene/air diffusion flames, Comb. Flame 175 (2017) 270-282.

[15] M. Alden, A. Omrane, M. Richter, G. Sarner, Thermographic phosphors for thermometry: A survey of combustion applications, Prog. Ener. Combust. Sci. 37 (2011) 422-461.

[16] X. Liu, G. Zhang, Y. Huang, Y. Wang, F. Qi, Two-dimensional temperature and carbon dioxide concentration profiles in atmospheric laminar diffusion flames measured by mid-infrared direct absorption spectroscopy at 4.2 μm, Appl. Phys. B (2018) 124:61.

[17] N. J. Kempema, M. B. Long, Boundary condition thermometry using a thermographic-phosphor-coated thin filament, Appl. Opt. 55 (2016) 4691-4697.

[18] M. D. Smooke, R. J. Hall, M. B. Colket, J. Fielding, M. B. Long, C. S. McEnally, L. D. Pfefferle, Investigation of the transition from lightly sooting towards heavily sooting co-flow ethylene diffusion flames, Combust. Theory Modelling 8 (2004) 593-606.

[19] P. B. Kuhn, B. Ma, B. C. Connelly, M. D. Smooke, M. B. Long, Soot and thin-filament pyrometry using a color digital camera, Proc. Combust. Inst. 33 (2011) 743-750.

[20] M. D. Smooke, M. B. Long, B. C. Connelly, M. B. Colket, R.J. Hall, Soot formation in laminar diffusion flames, Combust. Flame, 143 (2005) 613-628.

[21] A. Satija, X. Huang, P. P. Panda, R.P. Lucht, Vibrational CARS thermometry and one-dimensional simulations in laminar H2/air counter-flow diffusion flames, Int. J. Hydrogen Ener. 40 (2015) 10662-10672.

[22] S. P. Kearney, M. N. Jackson, Dual-pump coherent anti-Stokes Raman scattering thermometry in heavily sooting flames, AIAA J. 45 (2007) 2947-2956.

[23]S. P. Kearney, T. W. Grasser, Laser-diagnostic mapping of temperature and soot statistics in a 2-m diameter turbulent pool fire, Combust. Flame 186 (2017) 32-44.

[24] D. Han, A. Satija, J. Kim, Y. Weng, J. P. Gore, R. P. Lucht, Dual-pump vibrational CARS measurements of temperature and species concentrations in turbulent premixed flames with CO2 addition, Combust. Flame 181 (2017) 239-250.

[25] N. J. Kempema, B. Ma, M. B. Long, Investigation of in-flame soot optical properties in laminar coflow diffusion flames using thermophoretic particle sampling and spectral light extinction, Appl. Phys. B (2016) 122:232.

[26] R.E. Palmer, The CARSFT computer code calculating coherent anti-Stokes Raman spectra: User and programmer information, Sandia National Labs., Livermore, CA (USA), 1989.

[27] A.D. Cutler, G. Magnotti, CARS spectral fitting with multiple resonant species using sparse libraries, J. of Raman Spectrosc. 42 (2011) 1949-1957.
[28] A. Satija, S. Yuan, S.V. Naik, R.P. Lucht, Vibrational CARS thermometry and one-dimensional numerical simulations in CH4/H2/air partially-premixed flames, Int. J. Hydrogen Ener. 40 (2015) 6959-6969.
[29] R. P. Lucht, V. Velur-Natarajan, C. D. Carter, K. D. Grinstead, J. R. Gord, P. M. Danehy, G. J. Feichtner, R. L. Farrow, Dual-pump coherent anti-Stokes Raman scattering temperature and CO_2 concentration measurements, AIAA J. 4 (2013) 679-686.